

# Surface Impedance Measurements of Cuprate Superconductors: $\text{Nd}_{1.85}\text{Ce}_{0.15}\text{CuO}_{4-\delta}$ —A Case Study

Steven M. Anlage,<sup>1</sup> Dong-Ho Wu,<sup>1</sup> Jian Mao,<sup>1</sup> Sining Mao,<sup>1</sup> X. X. Xi,<sup>1</sup> T. Venkatesan,<sup>1</sup> J. L. Peng,<sup>1</sup> and R. L. Greene<sup>1</sup>

Received 31 July 1993

We present results on the temperature dependence of the surface impedance of high-quality thin films and single crystals of the electron-doped  $\text{Nd}_{1.85}\text{Ce}_{0.15}\text{CuO}_{4-\delta}$  cuprate superconductor. Surprisingly, these measurements are consistent with the behavior of an *s*-wave BCS superconductor. We also briefly review some highlights of surface impedance measurements on hole-doped cuprate superconductors, and contrast those with the results on  $\text{Nd}_{1.85}\text{Ce}_{0.15}\text{CuO}_{4-\delta}$ .

**KEY WORDS:** Surface impedance; Nd-Ce-Cu-O; surface resistance; magnetic penetration depth.

## 1. INTRODUCTION

Our goal is to understand the nature and origin of superconductivity in oxide materials. The Meissner state electrodynamic response is one of the hallmarks of superconductivity. Historically, a great deal has been learned about conventional superconductors by examining their high-frequency electrodynamic properties. It is natural, therefore, to approach the problem of high-temperature superconductivity by probing these materials with time-varying electromagnetic fields and carefully studying the response of the superconductor to these external perturbations.

The surface impedance of a conductor is a measure of its response to an electromagnetic field. For a sufficiently thick material at low enough frequencies, the response of a conductor to a plane-wave electromagnetic signal can be characterized in terms of the ratio of electric and magnetic fields parallel to the surface, evaluated at the surface, [1]:

$$Z_s = E_{\parallel}(0)/H_{\parallel}(0)$$

The surface impedance is usually thought of in terms

of its real (lossy) and imaginary (inductive reactive) components:

$$Z_s(T, \omega) = R_s(T, \omega) + iX_s(T, \omega)$$

where, for a sufficiently thick superconductor, the surface reactance,  $X_s(T, \omega) = \mu_0 \omega \lambda_L(T)$ , and  $\lambda_L(T)$  is the London penetration depth. Physically, in a sufficiently pure superconductor, the surface resistance  $R_s$  is sensitive to absorption of radiation by quasi particles and by Cooper pairs bound by an energy less than  $\hbar\omega$ , and  $X_s$  is sensitive to the inductive reactance of the condensed Cooper pairs.

## 2. SUMMARY OF PAST WORK ON HOLE-DOPED CUPRATES

The  $\text{YBa}_2\text{Cu}_3\text{O}_{7-\delta}$  (YBCO) and  $\text{Bi}_2\text{Sr}_2\text{CaCu}_2\text{O}_8$  (Bi2212) materials have been the most extensively studied because of the abundance of high-quality thin films and single crystals. Both of these materials are hole-doped cuprates with closely spaced pairs of Cu-O planes in the crystal structure, and relatively short in-plane coherence lengths  $\xi_{ab} \sim 10\text{--}15 \text{ \AA}$  for YBCO and  $\xi_{ab} \sim 8\text{--}10 \text{ \AA}$  for Bi2212.

### 2.1. Early Measurements

The early measurements of the surface impedance of *c*-axis YBCO films were characterized by high

<sup>1</sup>Maryland Center for Superconductivity Research, Physics Department, University of Maryland, College Park, Maryland 20742.

residual losses and strong polynomial temperature dependences of  $R_s$  and  $\lambda$  [2–4]. The surface resistance and penetration depth were seen to drop rapidly below  $T_c$ , as expected of a BCS  $s$ -wave superconductor. However, this behavior changed markedly at approximately 80% of  $T_c$ , after which  $\delta R_s(T)$ ,  $\delta\lambda(T) \sim T$  or  $T^2$  typically. Residual losses at 4.2 K and scaled to 10 GHz were in the range of approximately  $100 \mu\Omega$  [3,5] in the best  $c$ -axis YBCO films. A number of groups found that these measurements were highly sensitive to the microstructure of the materials studied [6,7], with a clear progression of improvement from ceramic, to polycrystalline film, to oriented film, to single-crystal samples. However, all measurements were characterized by high residual losses for  $T < 0.8T_c$  (compared to the expectations of BCS theory).

Early measurements of the penetration depth in YBCO crystals were found to be largely consistent with  $s$ -wave BCS theory [8].

## 2.2. Later Measurements

With time, more systematic studies of the microstructure dependence of the surface impedance were performed. Laderman *et al.* correlated residual losses with dc transport properties and the density of high-angle grain boundaries in  $c$ -axis YBCO thin films on MgO substrates [9]. The highest-quality thin films, as determined from dc properties and high-angle grain boundary density, to this day have the lowest residual resistances observed in YBCO,  $R_s(4.2 \text{ K}, 10 \text{ GHz}) \sim 15 \mu\Omega$ , but still retain the polynomial temperature dependences  $\delta R_s(T) \sim T$ ,  $\delta\lambda(T) \sim T^2$ , for  $T < 0.75T_c$ . Residual inductivity was also found to scale with the dc properties of the films [10,11]. Quantitative fits to the temperature and frequency dependence of the residual surface impedance of YNCO  $c$ -axis films were obtained based upon the weakly coupled grain model [9,12,13].

## 2.3. Recent Measurements

Recently, detailed measurements on available YBCO films report that  $\delta\lambda(T) \sim T^2$ , while  $\delta R_s(T) \sim T$ , with  $\lambda(T)$  going into a flatter temperature dependence below approximately 10 K [14]. Similar results are obtained for  $\lambda(T)$  on Bi2212 crystals [14]. Measurements on YBCO crystals grown at the University of British Columbia show a striking  $\delta R_s(T) \sim T$  and  $\delta\lambda(T) \sim T$  behavior at low temperatures [15,16]. It was also found that crystals which

show linear-in- $T$  dependence of the penetration depth also have residual surface resistances of roughly  $75 \mu\Omega$  at 10 GHz, somewhat higher than thin films of YBCO (mentioned above) at the same temperature and frequency. These results on YBCO crystals are explained in terms of a rapidly decreasing quasi particle scattering rate below  $T_c$ , and a strong linear-in- $T$  dependence of the normal fluid density at low temperatures in the crystals. Another group has reported unconventional behavior in  $\lambda(T)$  in Tl2122 crystals [17].

The differences in  $\lambda(T)$  temperature dependences and in residual resistance between YBCO crystals and films have been attributed to the greater quenched disorder in the films. The disorder in films limits the decrease in the scattering rate below  $T_c$ , resulting in a decrease in the residual resistance [15,18]. Experiments in which Zn was doped into YBCO crystals show that the residual resistance decreased with increasing Zn content up to at least 0.3% Zn [18]. It was concluded that some defects are required in YBCO to achieve the lowest possible surface resistance.

No single surface impedance measurement has conclusively demonstrated, beyond any reasonable doubt, the intrinsic pairing state symmetry of the cuprate superconductors. A resolution of this question will only come after all extrinsic effects are understood, and a body of evidence of reproducible measurements on a variety of cuprates is obtained.

## 3. Nd–Ce–Cu–O

$\text{Nd}_{1.85}\text{Ce}_{0.15}\text{CuO}_{4-\delta}$  (NCCO) is a relatively simple cuprate from the standpoint of its crystal structure and superconducting properties. Our intention is to carefully study this simpler material to complement the surface impedance data which has been accumulated on the high- $T_c$  hole-doped cuprates. Because the crystal structure of NCCO at the optimum doping for superconductivity is tetragonal, there is no twinning present in these samples. Also, since there are no other conducting layers besides the copper–oxygen planes, there is no significant interruption of the conduction paths as is found, for instance, in twinned YBCO samples. NCCO has also a single copper–oxygen plane per unit cell, so there are no complications from interplanar transitions, as well as fewer opportunities to introduce stacking faults when the material is grown from the vapor or liquid phase. Finally, since the in-plane coherence length is substantially larger in NCCO [ $\xi_0 \sim 80 \text{ \AA}$ ] as compared to YBCO and Bi2212

[ $\xi_0 \sim 15 \text{ \AA}$ ], one would expect this material to be much less susceptible to the effects of weakly coupled grains on the electrodynamic properties. However, NCCO is thought to be more anisotropic than YBCO, and has substantially lower critical current densities at the same reduced temperature [19,20]. Hence, the effects of weakly coupled grains may still be present in the NCCO films. NCCO is simple, yet it retains the basic ingredients of cuprate superconductivity: the copper–oxygen plane, along with all of the unusual magnetic properties found at low doping in the cuprates.

NCCO samples were prepared in both thin-film and single-crystal form. Thin films have been grown by pulsed laser deposition in an  $\text{N}_2\text{O}$  atmosphere. Substrates used include  $\text{LaAlO}_3$  (LAO) (NCCO film thickness  $\sim 5000 \text{ \AA}$ ) and Yttria-stabilized Zirconia (YSZ)-buffered sapphire substrates (NCCO film thickness  $\sim 2600 \text{ \AA}$ ). Details of the film growth procedure and microstructure analysis are in the literature [19,20]. Single crystals were grown by the directional solidification technique, also documented extensively in the literature [21]. A great deal is known about the microstructure of our NCCO samples. First, there is no superlattice modulation observed in either the thin films or single crystals studied. The films grow in the T' phase with the  $c$ -axis normal to the substrate. No other orientations of grains were found in either X-ray diffraction or cross-sectional and plan-view TEM [22]. X-ray phi scans show no evidence [23] of the  $45^\circ$  misoriented grains which are so abundant, and correlated with high residual losses, in YBCO [9]. Also, X-ray rocking curve measurements show the in-plane misorientation between grains to be less than  $0.4^\circ$ , also quite good compared to YBCO films, [23]. RBS channeling yields on the films are as low as 9%, indicative of good quality, but not quite as good as the best YBCO films which show a 3% channeling yield. The high channeling yield is indicative of a greater density of point defects in NCCO films as compared to YBCO films. The only impurity phase indentified in the films is  $\text{Nd}_{0.5}\text{Ce}_{0.5}\text{O}_{1.75}$ (NCO), which is a nominally insulating material present at the 2% volume level, or below [22]. Note that all measurements on thin films were performed on as-prepared samples.

For single-crystal samples of NCCO it was found that the as-grown samples showed multiple superconducting transitions. A procedure was developed to etch the crystals in HCl, and anneal them to homogenize the oxygen and cerium distributions. Upon several iterations of this procedure, the crystals showed

very sharp single-phase superconducting transitions with  $T_c$ 's slightly higher than those of the thin film samples [24].

The microwave measurements were performed in a cylindrical superconducting Nb cavity with the sample perturbing the  $\text{TE}_{011}$  resonant mode. The sample was positioned in the center of the cavity on a sapphire hot-finger [25] which could be temperature-controlled independently of the Nb cavity. The background temperature dependence of the sapphire and substrate dielectric constant and loss tangent do not significantly influence the data presented here [24]. The RF magnetic fields are parallel to the Cu–O planes of the sample, producing shielding currents mainly in the Cu–O planes. Shielding from currents in the  $c$ -direction make a negligible contribution to the frequency shift and  $Q$  of the resonator.

It should be noted that the frequency shift,  $\delta f(T)$ , and change in quality factor,  $Q(T)$ , of the resonator are simply related to the changes in surface impedance of the sample [25]:

$$\delta f(T) \sim \delta \lambda(T), \quad \delta(1/Q(T)) \sim \delta R_s(T)$$

Also, the asymptotic low-temperature dependence of the surface impedance predicted by  $s$ -wave BCS theory is [1]

$$\begin{aligned} \delta \lambda(T) &\sim (1/T^{1/2}) e^{-\Delta(0)/k_B T}, \\ \delta R_s(T) &\sim (1/T) e^{-\Delta(0)/k_B T}, \quad \text{for } T < T_c/2 \end{aligned}$$

#### 4. RESULTS ON Nd–Ce–Cu–O

The residual surface resistance of NCCO crystals and NCCO films on LAO were found to be in the range of several milli-Ohms at 9.6 GHz and 2.2 K. This is typical of early samples of YBCO crystals and films. However, the temperature dependence of the magnetic penetration depth of these films and crystals shows very detailed agreement with the predictions of strong-coupled  $s$ -wave BCS theory. This is evident from the raw data alone (Fig. 1), where the change in penetration depth (proportional to the frequency shift of the resonant mode) with temperature is consistent with an activated behavior, the activation barrier being  $2\Delta(0)k_B T_c \sim 4.1$ . Note that activated behavior over the same energy gap is consistent with both the penetration depth change (frequency shift) and increase in surface resistance (shift in  $1/Q$ ). We also note that the activated behavior is essentially the same in both thin film and single-crystal data. To our knowledge, there is no other example of such

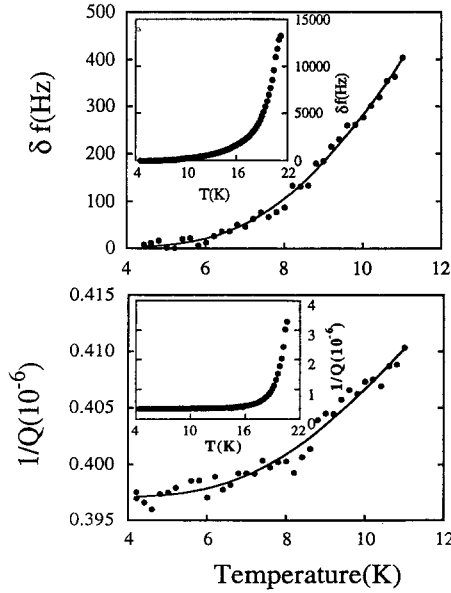


**Fig. 1.** Temperature dependence of  $\delta f$  and  $1/Q$  for  $T/T_c < 0.5$  for a NCCO thin film. The solid lines are the best fit to data which show  $\delta f(T) \sim (1/T^{1/2}) \exp\{-\Delta(0)/k_B T\}$  and  $\delta(1/Q(T)) \sim (1/T) \exp\{-\Delta(0)/k_B T\}$ , both with  $2\Delta(0)/k_B T_c = 4.1$ . Insets show  $\delta f$  and  $1/Q$  for the entire temperature range.

consistency in the temperature dependence of the electrodynamic properties for both films and crystals. Note that this same value for the energy gap was identified by tunneling measurements in the same class of NCCO crystal samples [26].

It should also be noted that the low-temperature frequency and  $1/Q$  shift can also be satisfactorily fitted to a dependence  $\delta f(T)$ ,  $\delta(1/Q(T)) \sim \alpha T + \beta T^2$ , which is the most general linear combination of dependences observed in YBCO and Bi2212 films and crystals (although we find that the parameter  $\alpha$  must be less than zero). In fact, one could argue quite generally in the context of  $d$ -wave pairing that linear-in- $T$  dependences are intrinsic, while quadratic dependences represent the effects of disorder on the nodes of the energy gap. Some may even argue that activated behavior should be observed in sufficiently disordered  $d$ -wave superconductors [27]. From this perspective, our fits of the low-temperature dependence of the surface impedance in NCCO to an activated behavior may not be conclusive evidence of an  $s$ -wave pairing state symmetry.

Examining our measurements at all temperatures,  $2.2 \text{ K} < T < T_c$ , we find that the data are also essentially consistent with the predictions of strong-coupled  $s$ -wave BCS theory [28]. Figures 2 and 3 show fits of the data for an NCCO thin film on LAO to the

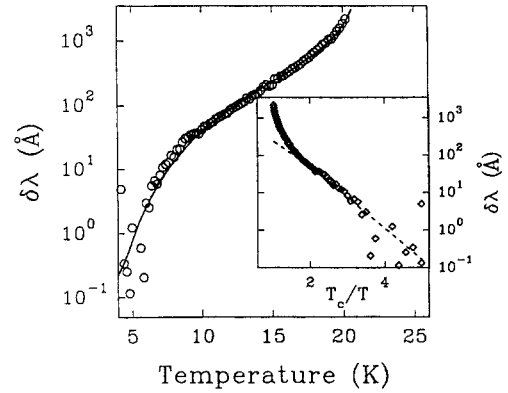


**Fig. 2.** Change in penetration depth  $\delta\lambda(T)$  at 9.6 GHz for a NCCO thin film. The solid line represents the BCS calculation with  $2\Delta(0)/k_B T_c = 4.1$ . Parameters used in the fit are given in Table I. Inset:  $\delta\lambda$  vs.  $T_c/T$ . Note the exponential behavior (dashed line)  $\delta\lambda(T) = \lambda(0) (\pi\Delta(0)/2k_B T)^{1/2} \exp\{-\Delta(0)/k_B T\}$  for  $T_c/T > 2$ .

$s$ -wave BCS temperature dependence of the surface impedance, while Table I shows values for the parameters used in the fits. The procedure for choosing these values is guided by other experiments on these films and crystals, and is discussed in detail in [24] and [29].

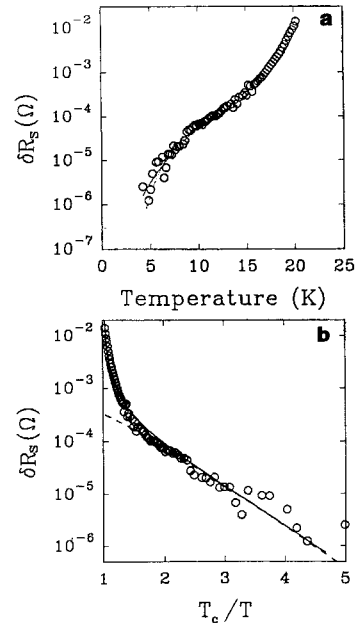


**Fig. 3.** (a)  $\delta R_s$  vs.  $T$  for a NCCO thin film at 9.6 GHz with a BCS calculation (solid line in both a and b). Parameters for the BCS fit are shown in Table I. (b)  $\delta R_s(T)$  vs.  $T_c/T$  with the exponential behavior (dashed line) of  $\delta R_s(T) \sim [(\hbar\omega)^2/k_B T] \ln(4k_B T/\hbar\omega) \exp\{-\Delta(0)/k_B T\}$  at low temperatures ( $T_c/T > 2$ ) with  $2\Delta(0)/k_B T_c = 4.1$ .

**Table I.** Electrodynamic Parameters Used to Fit the  $\lambda(T)$  and  $R_s(T)$  Data with the BCS Calculations for  $\text{Nd}_{1.85}\text{Ce}_{0.15}\text{CuO}_{4-\delta}$ <sup>a</sup>

Property	Thin films on $\text{LaAlO}_3$	Single crystal
$T_c$ (K)	21	21.5
$\lambda_{\parallel}(0)$ (Å)	$1300 \pm 100$	$1250 \pm 200$
$\xi_{\parallel}(0)$ (Å)	72-80	80
$R_0$ (mΩ)	2.5	1
$l_{\text{MFP}}$ (Å)	115-600	$300 \pm 200$
$2\Delta(0)/k_B T_c$	4-4.3	3.9-4.3
$\lambda_{L\parallel}(0)$ (Å)	$1000 \pm 90$	$1050 \pm 200$

<sup>a</sup>Parameters above the center line were determined by independent means, and those below the line were used as fitting parameters [24].

Recently we have examined NCCO films grown on YSZ-buffered sapphire substrates [29,30]. The results for the temperature dependence of the surface impedance are fully consistent with the results presented above. However, we found that the residual surface resistance at 9.6 GHz was reduced from the milli-Ohm range to below  $100 \mu\Omega$ , making them comparable in loss to typical YBCO films and crystals at 4.2 K.

## 5. DISCUSSION

We now compare and contrast these results on NCCO with the body of surface impedance data which exists on the hole-doped cuprates. The most striking difference is the degree of consistency in results on going from film to film and between films and crystals of NCCO. Such consistency is found mainly in the highest-quality films and crystals of YBCO, but is rarely found between the film and crystal samples of YBCO. Next, the temperature dependence of the surface impedance up to  $T_c$  is much more “conventional” than either YBCO or Bi2212. NCCO does not show the substantial deviations from the BCS temperature dependence which are seen in the hole-doped cuprates [12,15] (other than the existence of a residual loss). The fact that the residual losses have been substantially reduced with only modest effort also suggests that NCCO may become a useful low-loss, low- $T_c$  superconductor in the future, possibly competing with Ba-K-Bi-O and NbN in microwave applications [31].

Many questions remain to be answered about the surface impedance of the cuprates. Why do electrodynamic measurements on the other cuprates display non- $s$ -wave BCS behavior? Is it because they are

$d$ -wave superconductors, or are there a number of extrinsic effects which are very sensitive to microstructure? Why should NCCO look so much like traditional  $s$ -wave superconductors when it too is a *bona-fide* cuprate superconductor? Are defects and disorder playing a major role in the electrodynamics of the cuprate superconductors? We shall further address these questions, and discuss the contrast between NCCO and YBCO, in upcoming publications [29,30].

## 6. CONCLUSIONS

In summary, we have shown that the experimental surface impedance of NCCO films and crystals displays clear quantitative consistency with  $s$ -wave BCS theory. NCCO, in contrast with the hole-doped cuprates, behaves as if it had a single-valued and finite gap ratio throughout the entire temperature range below  $T_c$ . From this and other studies, it appears that NCCO has a superconducting state which is remarkably similar to that of conventional superconductors.

## ACKNOWLEDGMENTS

We thank P. Kneisel of CEBAF for his generous help with the Nb cavity. This work was supported by NSF Grant No. DMR-9123198, and an NSF NYI grant No. DMR-9258183, as well as the State of Maryland.

## REFERENCES

1. J. P. Turneaure, J. Halbritter, and H. A. Schwetman, *J. Supercond.* **4**, 341 (1991).
2. J. P. Carini, A. Awasthi, W. Beyermann, G. Grüner, T. Hylton, K. Char, M. R. Beasley, and A. Kapitulnik, *Phys. Rev. B* **37**, 9726 (1988).
3. T. Hylton, M. R. Beasley, A. Kapitulnik, J. Carini, L. Drabek, and G. Grüner, *IEEE Trans. Magn.* **25**, 810 (1989).
4. A. T. Fiory, A. F. Hebard, P. M. Mankiewich, and R. E. Howard, *Phys. Rev. Lett.* **61**, 1419 (1988); J. Annett, N. Goldenfeld, and S. R. Renn, *Phys. Rev. B* **43**, 2778 (1991).
5. H. Piel and G. Müller, *IEEE Trans. Magn.* **MAG-27**, 854 (1991).
6. L. Drabek, K. Holczer, G. Grüner, J. Chang, D. J. Scalapino, A. Inam, X. D. Wu, L. Nazar, and T. Venkatesan, *Phys. Rev. B* **42**, 10020 (1990).
7. Dong-Ho Wu, W. L. Kennedy, C. Zahopoulos, and S. Sridhar, *Appl. Phys. Lett.* **55**, 696 (1989).
8. L. Krusin-Elbaum, R. L. Greene, F. Holtzberg, A. P. Malozemoff, and Y. Yeshurun, *Phys. Rev. Lett.* **62**, 217 (1989).
9. S. S. Laderman, R. C. Taber, R. D. Jacowitz, J. L. Moll, C. B. Eom, T. L. Hylton, A. F. Marshall, T. H. Geballe, and M. R. Beasley, *Phys. Rev. B* **43**, 2922 (1991).

10. S. M. Anlage, B. W. Langley, J. Halbritter, C. B. Eom, N. Switz, T. H. Geballe, and M. R. Beasley, *MRS Symposium Proceedings*, Vol. 195, G. D. Cody, P. Sheng, and T. H. Geballe, eds.
11. C. B. Eom, J. Z. Sun, B. M. Lairson, S. K. Streiffer, A. F. Marshall, K. Yamamoto, S. M. Anlage, J. C. Bravman, T. H. Geballe, S. S. Laderman, R. C. Taber, and R. D. Jacowitz, *Physica C* **171**, 354 (1990).
12. S. M. Anlage, B. W. Langley, G. Deutscher, J. Halbritter, and M. R. Beasley, *Phys. Rev. B* **44**, 9764 (1991).
13. D. Miller, P. L. Richards, S. Etemad, A. Inam, T. Venkatesan, B. Dutta, X. D. Wu, C. B. Eom, T. H. Geballe, N. Newman, and B. F. Cole, *Phys. Rev. B* **47**, 8076 (1993).
14. M. R. Beasley, *Physica C* **209**, 43 (1993); Z. Ma, R. C. Taber, L. W. Lombardo, A. Kapitulnik, M. R. Beasley, P. Merchant, C. B. Eom, S. Y. Hou, and J. M. Phillips, *Phys. Rev. Lett.* **71**, 781 (1993).
15. D. A. Bonn, P. Dosanjh, R. Liang, and W. N. Hardy, *Phys. Rev. Lett.* **68**, 2390 (1992).
16. W. N. Hardy, D. A. Bonn, D. C. Morgan, R. Liang, and K. Zhang, *Phys. Rev. Lett.* **70**, 3999 (1993).
17. H. Ning, H. Duan, P. D. Kirven, A. M. Hermann, and T. Datta, *J. Supercond.* **5**, 503 (1992).
18. K. Zhang, D. A. Bonn, R. Liang, D. J. Baar, and W. N. Hardy, *Appl. Phys. Lett.* **62**, 3019 (1993).
19. S. N. Mao, X. X. Xi, S. Bhattacharya, Q. Li, T. Venkatesan, J. L. Peng, R. L. Greene, J. Mao, D. H. Wu, and S. M. Anlage, *Appl. Phys. Lett.* **61**, 2356 (1992).
20. S. N. Mao, X. X. Xi, S. Bhattacharya, Q. Li, J. L. Peng, J. Mao, D. H. Wu, S. M. Anlage, R. L. Greene, and T. Venkatesan, *IEEE Trans. Appl. Supercond.* **3**, 1552 (1993).
21. J. L. Peng, Z. Y. Li, and R. L. Greene, *Physica C* **177**, 79 (1991).
22. D. P. Beesabathina, L. Salamanca-Riba, S. N. Mao, X. X. Xi, and T. Venkatesan, *Appl. Phys. Lett.* **62**, 3022 (1993).
23. S. N. Mao, X. X. Xi, Q. Li, T. Venkatesan, D. Beesabathina, L. Salamanca-Riba, and X. D. Wu, *J. Appl. Phys.* (Feb. 15, 1994).
24. Dong-Ho Wu, Jian Mao, S. N. Mao, J. L. Peng, X. X. Xi, T. Venkatesan, R. L. Greene, and S. M. Anlage, *Phys. Rev. Lett.* **70**, 85 (1993).
25. S. Sridhar and W. Kennedy, *Rev. Sci. Instrum.* **59**, 531 (1988); W. L. Kennedy, Ph.D. Thesis, Northeastern University, 1990.
26. Q. Huang, J. F. Zasadzinski, N. Talshawala, K. E. Gray, D. G. Hinks, J. L. Peng, and R. L. Greene, *Nature (London)* **347**, 369 (1990).
27. P. Lee, *Phys. Rev. Lett.* **71**, 1887 (1993).
28. J. Halbritter, *Z. Phys.* **266**, 209 (1974).
29. S. M. Anlage, Dong-Ho Wu, Jian Mao, S. N. Mao, J. L. Peng, X. X. Xi, T. Venkatesan, and R. L. Greene, submitted to *Phys. Rev. B*.
30. S. N. Mao, X. X. Xi, J. Mao, D. H. Wu, Q. Li, S. M. Anlage, T. Venkatesan, D. Beesabathina, L. Salamanca-Riba, and X. D. Wu, *Appl. Phys. Lett.* **64**, 375 (1994).
31. M. Pambianchi, S. M. Anlage, E. S. Hellman, E. H. Hartford, M. Bruns, and S. Y. Lee, *Appl. Phys. Lett.* **64**, 244 (1994).